

## Optical–Optical Double-Resonance Spectroscopy of BaF: The $E^2\Sigma^+$ and $F^2\Pi$ States

PRECILA C. F. IP, PETER F. BERNATH, AND ROBERT W. FIELD

*Department of Chemistry and Spectroscopy Laboratory, Massachusetts Institute of Technology,  
Cambridge, Massachusetts 02139*

Sub-Doppler optical–optical double-resonance excitation spectra of BaF were recorded using two single-mode cw dye lasers. In the 30 000-cm<sup>-1</sup> region, the electronic states observed were  $E^2\Sigma^+$  and  $F^2\Pi$ . The latter had been previously assigned as the “ $F^2\Sigma^+$ ” state by Fowler [*Phys. Rev.* **59**, 645–652 (1941)]. The (3, 0) and (4, 0) bands of the  $E^2\Sigma^+ - B^2\Sigma^+$  transition and the (1, 0) and (2, 0) bands of the  $F^2\Pi - B^2\Sigma^+$  transition were rotationally analyzed. The molecular constants suggest inferences about the dominant atomic orbital character of the Rydberg molecular orbitals responsible for the  $E^2\Sigma^+$  and  $F^2\Pi$  electronic states. A new electronic state, the  $E' \ ^2\Pi$ , is predicted. The molecular parameters obtained (in cm<sup>-1</sup>, 1 $\sigma$  uncertainty in parentheses) are

	$v'_k$	$E^2\Sigma^+$	$v'_l$	$F^2\Pi$
$T_{v'0}$	3	29 767.32(1)	1	29 997.29(1)
$\Delta G_{v'+1/2}$	3	522.841(27)	1	522.553(2)
$B_e$		0.22990(22)		0.22931(8)
$\alpha_e$		0.00113(14)		0.00108(2)
$A_{v'}$			1	56.9840(12)
$p_{v'}$			1	-0.02426(6)
$\gamma_{v'}$	3	-0.17367(46)		

### I. INTRODUCTION

Barium fluoride is of interest because it should be possible to represent the Ba<sup>+</sup>F<sup>-</sup> molecule by a one-electron hydrogenic model. The electronic states arise from excitation of the single nonbonding electron to higher-lying orbitals. Some of these electronic states can be arranged into Rydberg series and it is particularly interesting to determine which Rydberg orbitals are responsible for the observed electronic states.

In order to study the electronic spectrum of barium monofluoride, we have used the technique of optical–optical double-resonance (OODR) excitation spectroscopy (1). As the name indicates, the method employs two visible-wavelength photons: the wavelength of the first photon is adjusted to excite the molecule to an intermediate state, then the wavelength of the second photon is scanned, thus probing high-lying states in the region 3.5–4.5 eV above  $X^2\Sigma^+$ . When the wavelength of the second photon is tuned onto resonance, an ultraviolet fluorescence signal can be detected.

This technique not only gives access to high-lying electronic states, but it also results in sub-Doppler linewidths. Furthermore, the excitation spectra are free of

overlap, which makes rotational assignment a trivial task. The major drawback is that the method is time consuming because a large number of  $1\text{-cm}^{-1}$  scans must be taken and the frequency of each line measured precisely relative to the  $I_2$  spectrum in order to characterize an electronic state.

In the present OODR experiments, the first laser excited the  $B^2\Sigma^+-X^2\Sigma^+$  transition of BaF. While the frequency of the first laser was held fixed, the frequency of the second laser was scanned and the undispersed uv fluorescence was monitored. The resultant OODR excitation spectra included transitions from  $v = 0$  of  $B^2\Sigma^+$  into  $v = 3, 4$  of the  $E^2\Sigma^+$  and  $v = 1, 2$  of the  $F^2\Pi$  state. The  $F^2\Pi$  state had been previously labeled as a  $^2\Sigma^+$  state (2). These two states were rotationally analyzed and molecular constants were generated in a nonlinear, direct-approach, least-squares fit (3).

## II. EXPERIMENTAL DETAILS

The first laser was a  $Kr^+$ -pumped Coherent Model CR599-21 continuous wave dye laser using Oxazine 725 dye. The second laser was an  $Ar^+$ -pumped CR599-21 with either rhodamine 6G or 101 dye. Single-mode dye laser output powers were about 50 mW with 3 W all lines pump power (all lines  $Kr^+$  red for Oxazine, all lines  $Ar^+$  for rhodamines). Beams from the two dye lasers were made to overlap with a beamsplitter (throwing away 50% of each beam) and were focused by a 30-cm focal length lens into a Broida-type oven (4). The BaF molecule was produced by the reaction  $Ba + SF_6$  with argon as carrier gas. Typical oven conditions were 0.5 Torr of Ar carrier gas with <1% oxidant injected concentrically to the Ba + Ar flow outside of the oven chamber.

Frequency calibration of the first laser was accomplished using a Ne pen lamp. For the second laser, an excitation spectrum from an  $I_2$  reference cell and frequency markers from a 750-MHz semiconfocal Fabry-Perot etalon were recorded simultaneously with the OODR excitation spectrum. The absolute uncertainty in the measured OODR lines was about  $0.004\text{ cm}^{-1}$  using the  $I_2$  atlas of Gerstenkorn and Luc (5). The measured lines and derived band origins were *not* corrected by subtraction of  $0.0056\text{ cm}^{-1}$  (6).

The first laser populated a selected  $v', J'$ , parity level of the  $B^2\Sigma^+$  state. Red  $B-X$  fluorescence was monitored with a Hamamatsu R818 photomultiplier through a Hoya R70 filter which passed fluorescence with  $\lambda > 7000\text{ \AA}$ . The specific  $B^2\Sigma^+$   $v = 0$  level excited was identified by comparing the measured laser frequency against the  $B-X$  (0, 0) band calculated using the constants of Ref. (7). These assignments were subsequently confirmed by  $B$ -state combination differences in the OODR spectra.

While the frequency of the first laser was held fixed, the second laser was scanned and uv fluorescence was monitored through a Corning 7-54 filter by a Hamamatsu R212 photomultiplier tube. For each level populated by the first laser, a series of  $1\text{-cm}^{-1}$  scans were made in order to obtain both the main line and several satellite lines, which resulted from  $J$ -changing collisions in the intermediate  $B$  state.

## III. RESULTS

Lines observed in the OODR excitation spectra were rotationally assigned simply by counting within a branch to the main OODR line, for which  $B$ -state

TABLE I

BaF  $F^2\Pi-B^2\Sigma^+$  (2, 0) Observed and Calculated Line Positions ( $\text{cm}^{-1}$ )<sup>a</sup>

J	$P_{21ee}(J)$	$Q_{21fe}(J)$	$R_{21ee}(J)$	J	$P_{12ff}(J)$	$Q_{12fe}(J)$	$R_{12ff}(J)$
1.5			16 509.417(-3)	1.5			
2.5	16 507.682(-3)	16 508.720(-3)		2.5			
3.5	507.608(-3)	509.200(-4)	511.255(3)	3.5	16 448.332(1)	16 449.997(-1)	
4.5	507.676(-2)	509.722(-4)	512.227(-2)	4.5	447.696(1)	449.838(1)	16 452.185(1)
5.5	507.782(-4)	510.285(-3)	513.238(-8)	5.5	447.095(-2)	449.715(1)	452.490(1)
6.5	507.929(-6)	510.892(1)		6.5	446.536(1)	449.629(1)	452.633(4)
7.5	508.121(-1)	511.536(1)	515.404(1)	7.5	446.012(2)	449.578(-1)	453.211(3)
8.5	508.351(-1)	512.218(-2)		8.5	445.526(4)	449.568(1)	453.627(5)
9.5	508.619(-3)	512.946(1)		9.5		449.593(1)	
10.5	508.931(-3)	513.711(-1)		10.5		449.655(1)	
11.5	509.283(-3)	514.520(2)		11.5	444.279(-2)	449.756(3)	
12.5	509.676(-3)	515.367(2)	521.514(6)	12.5	443.940(-2)	449.891(2)	
13.5	510.108(-4)			13.5	443.641(1)		
14.5	510.584(-2)		524.233(-2)	14.5			
15.5	511.105(4)			15.5			
16.5	511.656(-1)	519.168(5)		16.5	442.955(-1)		
17.5	512.258(4)	520.217(3)		17.5	442.803(1)		
18.5	512.896(5)	521.308(2)		18.5	442.685(-1)		
19.5	513.574(4)	522.441(2)	531.765(2)	19.5	442.607(-1)		
20.5	514.293(4)	523.612(1)	533.392(1)	20.5	442.564(-2)		
21.5			535.064(5)	21.5	442.564(2)		
22.5	515.049(-1)	526.076(-5)	536.772(4)	22.5	442.596(1)		
23.5			538.518(-1)	23.5	442.655(-1)		
24.5				24.5	442.773(1)		
25.5	519.502(2)			25.5	442.918(-1)		
26.5	519.470(7)			26.5		455.702(2)	
27.5				27.5		456.400(5)	
28.5				28.5	443.581(-1)	457.131(3)	
29.5	522.605(3)			29.5	443.880(3)	457.894(-4)	
30.5				30.5	444.207(-4)		
33.5				33.5	445.443(4)		
34.5				34.5	445.923(-1)		
35.5				35.5	446.446(-1)		
39.5				39.5			
40.5				40.5			

J	$P_{2ff}(J)$	$Q_{2ef}(J)$	$R_{2ff}(J)$	J	$P_{1ee}(J)$	$Q_{1fe}(J)$	$R_{1ee}(J)$
1.5				1.5			
2.5			16 508.281(-2)	2.5			
3.5			508.541(-2)	3.5			
4.5		16 506.342(3)	508.851(9)	4.5			16 455.714(-4)
5.5	16 503.729(8)	506.226(1)	509.188(6)	5.5			456.721(-3)
6.5	503.201(9)	506.154(3)	509.571(8)	6.5			457.769(3)
7.5			509.981(-4)	7.5			458.849(3)
8.5		506.124(-1)	510.445(-3)	8.5		16 455.438(-4)	
9.5		506.177(4)	510.954(3)	9.5		456.121(2)	
10.5		506.265(2)	511.496(1)	10.5		456.833(-1)	
11.5			512.079(-1)	11.5		457.587(1)	
12.5				12.5		458.381(7)	464.793(-4)
13.5			513.375(4)	13.5			466.094(-4)
14.5				14.5			467.429(-7)
15.5		507.024(-2)		15.5			
16.5		507.316(-3)		16.5			
17.5		507.646(-7)	515.612(-1)	17.5	16 455.403(-3)		
18.5				18.5	455.908(-2)		
19.5		508.440(-3)		19.5	456.610(-2)	464.930(-3)	
20.5		508.897(-5)		20.5	457.266(-6)	466.015(-3)	
21.5		509.393(-4)		21.5	457.969(1)	467.138(-3)	
22.5		509.930(-4)		22.5	458.705(4)	468.300(-1)	
23.5		510.510(-4)	521.195(-3)	23.5			
24.5		511.135(1)	522.270(-2)	24.5			
25.5		511.791(-3)		25.5			
26.5				26.5			
27.5		513.238(-1)		27.5			
28.5				28.5			
29.5				29.5			
30.5		515.705(-7)		30.5			
33.5				33.5			
34.5				34.5			
35.5				35.5			
39.5				39.5		493.746(1)	
40.5				40.5		495.580(-1)	

<sup>a</sup>Number in parentheses is (observed calc.) in  $10^{-3} \text{ cm}^{-1}$ .

$v'' = 0, J''$ , and  $e/f$  parity were known from the selected  $B-X(0, 0)$  line (7). These assignments of  $E-B$  and  $F-B$  OODR lines were confirmed by obtaining constant  $B$ -values from upper-state combination differences. Assigned OODR lines for the  $F-B(2, 0)$  and  $(1, 0)$  and  $E-B(4, 0)$  and  $(3, 0)$  bands are listed in Tables I-IV.

A nonlinear least-squares approach was used in a direct simultaneous fit of all four  $E^2\Sigma^+(v = 3, 4)-B^2\Sigma^+(v = 0)$  and  $F^2\Pi(v = 1, 2)-B^2\Sigma^+(v = 0)$  OODR bands, using the line positions given in Tables I-IV. The standard  ${}^2\Pi-{}^2\Sigma$  Hamiltonian (8) was used and the  $v = 0$  level of the  $B$  state was chosen as the zero of energy because  $T_0(B^2\Sigma^+)$  was known less well (7) than our OODR band origins. All parameters were allowed to vary except for  $B$ -state centrifugal distortion. Simultaneous fitting of all lines from all observed bands reduced correlations among the molecular parameters. It was necessary to include an  $A_D$  constant in the  ${}^2\Pi$

TABLE II

BaF  $F^2\Pi-B^2\Sigma^+$  (1, 0) Observed and Calculated Line Positions ( $\text{cm}^{-1}$ )<sup>a</sup>

J	$P_{21ee}(J)$	$Q_{21fe}(J)$	$R_{21ee}(J)$	J	$P_{12ff}(J)$	$Q_{12ef}(J)$	$R_{12ff}(J)$
5, 5				5, 5		15 927.186(-1)	
7, 5				7, 5		927.084(3)	
8, 5		15 989.767(4)		8, 5		927.084(-3)	
9, 5		990.509(1)		9, 5		927.129(-3)	
10, 5		991.259(2)		10, 5		927.215(-1)	
11, 5		992.127(1)		11, 5	15 921.843(-3)		
12, 5			15 999.170(-2)	12, 5		921.530(-1)	
13, 5			16 000.545(-2)	13, 5		921.253(-3)	
14, 5	15 988.250(-1)	994.879(3)	001.968(-4)	14, 5		921.017(-3)	
15, 5	988.798(2)			15, 5		920.821(-1)	
16, 5				16, 5		920.663(-1)	928.543(1)
17, 5	990.011(-5)			17, 5		920.546(1)	928.901(-1)
18, 5	990.685(-5)	999.136(-5)		18, 5		920.467(1)	929.300(1)
19, 5	991.404(-4)	16 000.313(-2)	009.683(-2)	19, 5		920.428(1)	929.736(1)
20, 5	992.169(1)	001.529(-1)		20, 5		920.428(2)	930.212(1)
21, 5		002.780(-1)		21, 5		920.467(2)	930.726(-1)
22, 5		004.088(-2)		22, 5		920.546(2)	931.284(3)
23, 5				23, 5		920.663(1)	931.871(-4)
24, 5				24, 5		920.821(1)	932.529(-1)
25, 5				25, 5		921.017(-1)	933.161(-1)
26, 5		009.727(4)		26, 5		921.253(-1)	933.891(-3)
27, 5				27, 5		921.530(1)	
28, 5				28, 5		921.843(-3)	
29, 5				29, 5			
30, 5				30, 5			
31, 5				31, 5		15 938.048(1)	
32, 5				32, 5		938.999(2)	
33, 5				33, 5			
34, 5				34, 5		941.013(-1)	
35, 5				35, 5			
36, 5				36, 5			
42, 5				42, 5			
43, 5				43, 5			

J	$P_{2ff}(J)$	$Q_{2ef}(J)$	$R_{2ff}(J)$	J	$P_{1ee}(J)$	$Q_{1fe}(J)$	$R_{1ee}(J)$
5, 5				5, 5			
7, 5		15 983.646(3)		7, 5			
8, 5		983.669(7)		8, 5			15 937.508(6)
9, 5		983.737(1)		9, 5			938.674(-4)
10, 5		983.849(2)		10, 5			939.896(4)
11, 5		984.002(1)		11, 5			941.148(3)
12, 5		984.201(2)	15 990.369(1)	12, 5			942.438(1)
13, 5			991.064(-1)	13, 5			
14, 5			991.807(4)	14, 5	15 931.515(-1)	15 937.736(-1)	
15, 5			992.587(1)	15, 5		938.674(3)	
16, 5				16, 5		932.559(-2)	939.646(3)
17, 5				17, 5		933.140(-3)	940.651(-3)
18, 5	15 977.826(2)			18, 5		933.763(-1)	941.700(-4)
19, 5	977.863(-1)	906.782(4)	996.146(5)	19, 5			942.793(-1)
20, 5	977.944(-4)	987.317(-1)	997.139(3)	20, 5			
21, 5	978.072(-1)	987.901(-1)		21, 5			
22, 5	978.242(-1)	988.525(-2)	999.252(-3)	22, 5			
23, 5			16 000.380(1)	23, 5			
24, 5		989.907(-1)	001.548(1)	24, 5			
25, 5		990.660(-2)	002.757(1)	25, 5	939.212(-1)		
26, 5		991.459(-1)	004.007(-1)	26, 5			
27, 5		992.302(1)		27, 5			
28, 5				28, 5			
29, 5				29, 5	943.194(1)		
30, 5	981.146(4)		009.449(4)	30, 5			
31, 5	981.700(2)			31, 5			
32, 5				32, 5			
33, 5				33, 5			
34, 5		999.388(-1)		34, 5			
35, 5				35, 5			
36, 5		16 001.005(5)		36, 5			
42, 5	990.660(3)			42, 5			
43, 5	991.724(-2)			43, 5			

<sup>a</sup>Number in parentheses is (observed-calc.) in  $10^{-3} \text{ cm}^{-1}$ .

Hamiltonian in order to obtain a satisfactory fit. Table V summarizes the resultant molecular constants.

Fowler's (2) vibrational numbering of the  $F^2\Pi$  state was confirmed by comparing observed relative intensities within the ( $v' = 1$  and 2,  $v''_X$ )  $F-X$  fluorescence progressions against calculated Franck-Condon factors.

Table VI lists the equilibrium constants of the  $F^2\Pi$  and  $E^2\Sigma$  states. Since only two bands of the  $F-B$  transition were analyzed, the Pekeris relationship (9) was used to estimate  $\omega_e$  and  $\omega_e x_e$  from the single measured  $\Delta G$  value. For the  $E^2\Sigma$  state, the Barrow *et al.* (7)  $T_0$  value was combined with the two measured  $E-B$  band origins to determine  $\omega_e$  and  $\omega_e x_e$  directly. The  $E$ - and  $F$ -state values for  $B_e$  and  $\alpha_e$  listed in Table VI were each determined from a single pair of  $B_v$  values. The extrapolated  $B_0 = 0.22934 \pm 0.00029 \text{ cm}^{-1}$  value for the  $E^2\Sigma$  state agrees with the value,  $0.2290 \text{ cm}^{-1}$ , obtained by Barrow *et al.* (7) from the  $E-X$  (0, 0) band.

TABLE III

BaF  $E^2\Sigma^+ - B^2\Sigma^+$  (4, 0) Observed and Calculated Line Positions ( $\text{cm}^{-1}$ )<sup>a</sup>

N	$P_1(N)$	$R_1(N)$
6		16 254.032(-1)
8		255.552(1)
41	16 263.982(1)	301.041(-2)
42	265.073(1)	303.023(-3)
43	266.200(2)	305.044(-1)
44	267.364(3)	
45		309.190(1)
N	$P_2(N)$	$R_2(N)$
3	16 248.550(3)	
7	247.336(-4)	16 254.262(7)
8	247.123(-3)	254.947(7)
9	246.949(1)	255.665(4)
10	246.803(-2)	256.422(5)
11	246.696(-2)	
12	246.620(-5)	
13	246.585(-3)	

<sup>a</sup>Number in parentheses is (obs.-calc.) in  $10^{-3}\text{cm}^{-1}$ .

## IV. DISCUSSION

## A. Intensity Anomalies

In Fowler's absorption spectrum he observed some weak bands which he thought, at first, to be from a  $^2\Pi - X^2\Sigma^+$  transition (2). But, because of the anomalous relative intensity of the two spin components in these bands, he ascribed them to two  $^2\Sigma^+ - ^2\Sigma^+$  transitions (2). Our excitation spectrum (Fig. 1) clearly showed two sets of  $P$ ,  $Q$ ,  $R$  triplets which could only belong to the two spin components of a  $^2\Pi$  state. Bandhead measurements from OODR spectra indicated that our  $F^2\Pi_{1/2} - X^2\Sigma$  heads occurred at the same wavelengths as Fowler's " $F^2\Sigma$ " state (2). We can offer no explanation for Fowler's observed  $F-X$  intensity anomalies. The value of  $\rho$  for  $F^2\Pi$  is too small for there to be substantial  $F^2\Pi_{1/2} \sim ^2\Sigma^+$  mixing.

TABLE IV

BaF  $E^2\Sigma^+ - B^2\Sigma^+$  (3, 0) Observed and Calculated Line Positions ( $\text{cm}^{-1}$ )<sup>a</sup>

N	$P_1(N)$	$R_1(N)$
14	15 725.436(1)	15 738.358(-3)
15		739.419(1)
N	$P_2(N)$	$R_2(N)$
19	15 724.672(1)	
20	724.923(-1)	15 743.608(-1)
21	725.214(-1)	744.798(-2)
22	725.544(2)	746.029(-1)
23	725.910(3)	

<sup>a</sup>Number in parentheses is (obs.-calc.) in  $10^{-3}\text{cm}^{-1}$ .

TABLE V  
 Constants for the  $F$ ,  $E$ , and  $B$  States of BaF ( $\text{cm}^{-1}$ )<sup>a</sup>

	$F^2\Pi$		$E^2\Sigma^+$		$B^2\Sigma^+$ <sup>b</sup>
	v=2	v=1	v=4	v=3	v=0
$\nu_0$	16 479.630(1)	15 957.077(1)	16 249.954(2)	15 727.113(25)	0.0
$B_v$	0.226605(11)	0.227686(8)	0.224823(13)	0.225948(127)	0.207202(7)
$D_v \times 10^6$	0.1537(25)	0.1697(19)	0.1553(41)	0.238(142)	0.1900 <sup>c</sup>
$A_v$	56.959(1)	56.984(1)	-	-	-
$A_{Dv} \times 10^4$	1.5678(244)	1.3320(260)	-	-	-
$\gamma_v$	-	-	-0.17080(23)	-0.17367(36)	-0.262903(27)
$P_v$	-0.02458(6)	-0.02426(6)	-	-	-
$q_v \times 10^4$	0.274(126)	-0.181(64)	-	-	-

<sup>a</sup>Number in parentheses is one standard deviation

<sup>b</sup> $T_0$  for  $B^2\Sigma^+ - X^2\Sigma^+$  is  $14\,040.21\text{cm}^{-1}$  (Ref. 7)

<sup>c</sup>Held fixed in the fit.

We observed anomalous  $R$  vs  $P$  intensities in the  $F^2\Pi_{1/2} - B^2\Sigma^+$  subband. These anomalies could be explained entirely on the basis of independently calculable mixing between the  $A^2\Pi_{1/2}$  and  $B^2\Sigma^+$  states. Using second-order perturbation theory and an estimate for the  $\{1/2\langle AL_+ \rangle + \langle BL_+ \rangle [1 \mp (J + 1/2)]\}$  perturbation matrix element ( $\delta$ ), the fractional character of  $A^2\Pi_{1/2}$  in  $B^2\Sigma^+$  was calculated to be about 4%. Assuming that the transition moments for  $F-B$  and  $F-A$  transitions are the same (cf. (10)), then the calculated intensities obtained from the equations given by Kopp and Hougen (11) agree satisfactorily with those observed.

### B. Rotational Energy Transfer

OODR linewidths and intensities provide information about rotational energy transfer (RET) in the intermediate electronic state ( $B^2\Sigma^+$ ). Collision-induced OODR satellite lines have larger (but still sub-Doppler) widths than those of the main lines because of velocity-changing collisions (VCC) (12). For initial  $B$ -state  $J$  values larger than 4.5 (RET from lower  $J$  levels was not examined), a strong  $|\Delta J|$  dependence of RET was observed. At 0.5 Torr and  $J_{\text{initial}} = 23.5$ , the relative intensities of main ( $\Delta J = 0$ ),  $|\Delta J| = 1$ , and  $|\Delta J| = 2$  lines are 10, 3, and 1, respectively. The expected short radiative lifetime of BaF  $B^2\Sigma^+$  (10) ensures that this is an approximately single-collision result.

In addition to the  $|\Delta J| = 1$  propensity rule, there was also an indication that  $e/f$  parity (13) is preserved in rotation-changing collisions. For example, if the first laser populates the  $e$  component of a given  $N$  level of  $B^2\Sigma^+$ , then the intensities of all  $f$ -component OODR lines are weaker than the  $|\Delta J| = 2 e \rightarrow e$  RET lines. The

TABLE VI  
 $E^2\Sigma$  and  $F^2\Pi$  Equilibrium Constants ( $\text{cm}^{-1}$ )<sup>a</sup>

	$E^2\Sigma$	$F^2\Pi$
$T_e$	28 139.4(10) <sup>b</sup>	29 440.7(10) <sup>b</sup>
$\omega_e$	539.08(10) <sup>c</sup>	529.81(70) <sup>d</sup>
$\omega_e x_e$	2.030(10)	-
$\omega_e x_e$ (Pekeris)	1.96(33)	1.815(45)
$B_e$	0.22990(22)	0.22931(8)
$\alpha_e$	0.00113(14)	0.00108(2)
$R_e$ ( $\text{\AA}$ )	2.096(1)	2.0982(4)

<sup>a</sup>Uncertainties in parentheses correspond to one standard deviation.

<sup>b</sup>Band head values of  $\omega_e'' = 468.9$  and  $\omega_e x_e'' = 1.79$  were used to obtain  $T_e$

[K. P. Huber and G. Herzberg, *Constants of Diatomic Molecules* (Van Nostrand, N.Y., 1979)]. The uncertainty reflects our estimated accuracy ( $\pm 1 \text{ cm}^{-1}$ ) of the band head  $\omega_e$  values.

<sup>c</sup>Barrow's  $T_0 = 28 174.45 \text{ cm}^{-1}$  for  $E^2\Sigma^+$  was used. [Ref. 7.]

<sup>d</sup>Calculated from  $\Delta G_{3/2}^+$  using Pekeris value of  $\omega_e x_e$ . The uncertainty reflects our estimated accuracy ( $\pm 10\%$ ) of the Pekeris  $\omega_e x_e$ .

same  $|\Delta J|$  and parity propensity rules were also observed in the  $A^2\Pi$  state of CaF (14). These propensity rules are consistent with first ( $|\Delta J| = 1, e \rightarrow e$ )- and second ( $|\Delta J| = 2, e \rightarrow e$ )-order  $MX$  electric dipole processes. The alkaline earth halides are excellent systems for detailed study of RET in the presence of nonzero electronic spin and orbital angular momenta, both because of their suitability to OODR and the relative ease of attaining single-collision conditions.

### C. Electronic Structure

An interesting trend in the molecular constants of BaF is that the rotational constants for excited electronic states are larger than those of the ground state. This decrease in internuclear distance at higher energy indicates that the "non-bonding" valence electron in  $\text{Ba}^+\text{F}^-$  is actually slightly antibonding at low energy.

Barrow *et al.* (7), on the basis of rotational analysis of the  $v = 0$  levels of BaF  $A^2\Pi$  and  $B^2\Sigma^+$ , concluded that these two states were in pure precession with each other and probably arose from  $6p\pi$  and  $6p\sigma$  orbitals, respectively.

Pure precession implies that (15)

$$p(^2\Pi) = \gamma(^2\Sigma^+) = \frac{2ABl(l+1)}{T_0(^2\Pi) - T_0(^2\Sigma^+)}$$

and suggests that the orbital angular momentum,  $l$ , of the nonbonding orbital is well defined with integral value. It seems reasonable to expect that, if the lowest excited states are in pure precession, then it ought to be possible to fit most of the higher excited states into pure precession relationships.

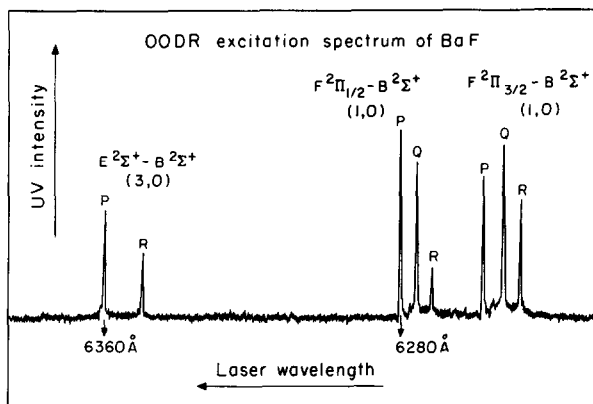


FIG. 1. OODR excitation spectrum of BaF using a single-mode first laser and a broadband second laser.

The  $\gamma$  and  $p$  values for  $E^2\Sigma^+$  and  $F^2\Pi$  are, respectively,  $-0.17$  and  $-0.024$   $\text{cm}^{-1}$ . Thus, for two reasons, the  $E$  and  $F$  states are not in simple pure precession with each other. First,  $p \neq \gamma$ . Second, the signs of  $\gamma$  and  $p$  imply that  $E^2\Sigma^+$  lies *above* its pure precession  $^2\Pi$  counterpart; similarly  $F^2\Pi$  lies *below* its  $^2\Sigma^+$  partner.

For the  $F^2\Pi$  state,  $A = 57$ ,  $B = 0.2288$ ,  $p = -0.025$ , and assuming  $l = 1$ ,  $T_0(^2\Pi) - T_0(^2\Sigma^+)$  is  $2100$   $\text{cm}^{-1}$ . Hence, the state that is in pure precession with  $F^2\Pi$  might be expected to lie near  $T_e = 31\,540$   $\text{cm}^{-1}$ . This value is close to  $T_e$  for the observed  $H^2\Sigma^+$  state ( $31\,582$   $\text{cm}^{-1}$ ), so that the  $F$  and  $H$  states are probably in pure precession and perhaps come from the  $8p\pi$  and  $8p\sigma$  orbitals, respectively. To verify this orbital assignment, a rotational analysis of the  $H^2\Sigma^+$  state must be performed in order to determine whether its  $\gamma$  parameter has the required pure precession value.

There is no known  $^2\Pi$  state with energy and  $A$  value suitable to qualify for pure precession with  $E^2\Sigma^+$ . Three possibilities exist:  $E^2\Sigma^+$  derives from an  $s$ ,  $p$ , or  $d$  orbital. The first possibility can be ruled out by the large value of  $\gamma$ . The second possibility requires<sup>1</sup> that the interacting  $7p\pi$   $E'$   $^2\Pi$  state lie between  $27\,000$  and  $28\,000$   $\text{cm}^{-1}$ . A  $d$  complex would locate<sup>1</sup> the  $nd$   $E'$   $^2\Pi$  state between  $25\,000$  and  $27\,000$   $\text{cm}^{-1}$ . A preliminary OODR experiment has located the  $v = 0$  level of a new  $^2\Pi_{3/2}$  state near  $27\,400$   $\text{cm}^{-1}$ . Before this new state and  $E^2\Sigma^+$  can be assigned as belonging to a  $7p$  orbital, the  $A$  and  $p$  values of the  $^2\Pi$  state must be determined.

## V. SUMMARY

The  $E^2\Sigma^+$  and  $F^2\Pi$  electronic states of the BaF molecule have been characterized by sub-Doppler OODR excitation spectroscopy. Tentative  $nl$  assignments are suggested for both states. Only a few definitive  $nl$  assignments will be required to enable arrangement of the electronic states of BaF into  $s$ ,  $p$ , and  $d$  Rydberg

<sup>1</sup> In order to estimate the location of the  $E'$   $^2\Pi$  state that interacts with  $E^2\Sigma^+$ , it is necessary to estimate its spin-orbit constant. Since  $E'$   $^2\Pi$  must lie between  $F^2\Pi$  and  $C^2\Pi$ , its  $A$  value should be bracketed by those of the  $F$  ( $57$   $\text{cm}^{-1}$ ) and  $C$  ( $200$   $\text{cm}^{-1}$ ) states. This range of  $A$  is reflected in the two quoted ranges for the energy of an  $l = 1$  or  $2$   $E'$   $^2\Pi$  state.

series and to provide a framework for meaningful comparisons between the electronic structure of  $Ba^+$  and the barium monohalides.

#### ACKNOWLEDGMENTS

Equipment for this research was provided by grants from the National Science Foundation (CHE78-10178) and the Air Force Office of Scientific Research (AFOSR-76-3056). P.F.B. was supported, in part, by a Natural Science and Engineering Research Council of Canada postgraduate fellowship and by AFOSR. P.C.F.I. was supported by a contract from the Air Force Geophysics Laboratory (F 19628-79-C-0123).

RECEIVED: October 17, 1980

#### REFERENCES

1. R. A. GOTTSCHO, J. B. KOFFEND, R. W. FIELD, AND J. R. LOMBARDI, *J. Chem. Phys.* **68**, 4110-4122 (1978).
2. C. A. FOWLER, *Phys. Rev.* **59**, 645-652 (1941).
3. R. N. ZARE, A. L. SCHMELTEKOPF, W. J. HARROP, AND D. L. ALBRITTON, *J. Mol. Spectrosc.* **46**, 37-66 (1973).
4. J. B. WEST, R. S. BRADFORD, J. D. EVERSOLE, AND C. R. JONES, *Rev. Sci. Instrum.* **46**, 164-168 (1975).
5. S. GERSTENKORN AND P. LUC, "Atlas du Spectre d'Absorption de la Molécule d'Iode CNRS," Paris, 1978.
6. S. GERSTENKORN AND P. LUC, *Rev. Phys. Appl.* **14**, 791-794 (1979).
7. R. F. BARROW, M. W. BASTIN, AND B. LONGBOROUGH, *Proc. Phys. Soc.* **92**, 518-519 (1967).
8. A. J. KOTLAR, R. W. FIELD, J. I. STEINFELD AND J. A. COXON, *J. Mol. Spectrosc.* **80**, 86-108 (1980).
9. G. HERZBERG, "Spectra of Diatomic Molecules," 2nd ed., p. 108, Van Nostrand-Reinhold, New York, 1950.
10. P. J. DAGDIGIAN, H. W. CRUSE, AND R. N. ZARE, *J. Chem. Phys.* **60**, 2330-2339 (1974).
11. I. KOPP AND J. T. HOUGEN, *Canad. J. Phys.* **45**, 2581-2596 (1967).
12. R. A. GOTTSCHO, R. W. FIELD, R. BACIS, AND S. J. SILVERS, *J. Chem. Phys.* **73**, 599-611 (1980).
13. J. M. BROWN, J. T. HOUGEN, K. P. HUBER, J. W. C. JOHNS, I. KOPP, H. LEFEBVRE-BRION, A. J. MERER, D. A. RAMSAY, J. ROSTAS, AND R. N. ZARE, *J. Mol. Spectrosc.* **55**, 500-503 (1975).
14. P. F. BERNATH AND R. W. FIELD, *J. Mol. Spectrosc.* **82**, 339-347 (1980).
15. R. S. MULLIKEN AND A. CHRISTY, *Phys. Rev.* **38**, 87-119 (1931).